# PHYSICAL REVIEW D

## PARTICLES AND FIELDS

THIRD SERIES, VOLUME 33, NUMBER 11 1 JUNE 1986


# Observation of $A$ dependence in Koba-Nielsen-Olesen scaling distributions for high-energy hadron-nucleus interactions


N. N. Biswas, S. J. Y. Ting, M. C. K. Mattingly, J. M. Bishop, N. M. Cason, V. P. Kenney, R. C. Ruchti, and W. D. Shephard

*University of Notre Dame, Notre Dame, Indiana 46556*

W. W. Neale, P. A. Elcombe, M. J. Goodrick, and J. C. Hill

*University of Cambridge, Cambridge CB3 0HE, England*

W. Kowald and W. D. Walker

*Duke University, Durham, North Carolina 27706*

P. Lucas and L. Voyvodic

*Fermilab, P.O. Box 500, Batavia, Illinois 60510*

R. Ammar, D. Coppage, R. Davis, D. Day, J. Gress, S. Kanekal, N. Kwak, and L. Herder

*University of Kansas, Lawrence, Kansas 66045*

J. Whitmore, R. A. Lewis, B. Y. Oh, G. A. Smith, and W. Toothacker

*Pennsylvania State University, University Park, Pennsylvania 16802*



(Received 2 July 1985)



Experimental multiplicity distributions scaled in the Koba-Nielsen-Olesen (KNO) form for hadron-nucleus interactions show clear deviations from the scaling distribution observed for hadron-hadron interactions. The deviations become larger as $A$ increases. Our data can be described by a model which invokes the hypothesis that KNO scaling is valid for hadron-nucleus interactions at a fixed impact parameter. In this model, the $A$ dependence of the multiplicity distributions results from the convolution of scatterings at various impact parameters.


## I. INTRODUCTION

The study of high-energy hadron-nucleus interactions is important as a possible source of information on the space-time development of hadronic interactions. One aspect of this study is the investigation of the multiplicity of "shower" particles produced in such interactions. There has been much discussion[1,2] on whether Koba-Nielsen-Olesen (KNO) scaling[3] holds for a nuclear target, and whether the shower-particle multiplicity distribution expressed in a KNO-scaled variable form is universal[4] for all nuclei. Recently a model has been proposed[5] which predicts a breakdown of KNO universality for hadron-nucleus interactions, more so for heavier nuclei, while retaining KNO universality at each impact parameter.

Experimental data on multiplicity distributions in high-energy hadron-nucleus interactions are rather scarce. Florian *et al.* and Azimov *et al.*[6] have reported emulsion data where the target nucleus is not uniquely known. Faessler *et al.*[7] have studied correlations of slow and fast particles. DeMarzo *et al.*[8] have recently studied KNO scaling using streamer-chamber data in which identification of protons could be achieved only up to a momentum of 0.6 GeV/$c$. The data presented here extend proton identification up to a momentum of 1.3 GeV/$c$ and are somewhat more extensive. The targets involved are Mg, Ag, and Au foils which were bombarded by 100-GeV/$c$ $p$, $\bar{p}$, $\pi^+$, $\pi^-$, and $K^+$ beams and a 320-GeV/$c$ $\pi^-$ beam. (The $K^+$ data are low in statistics and will not be presented in this paper.)

We present our experimental data in Sec. II. In Sec. III we investigate the question of KNO scaling in hadron-nucleus interactions and compare our data with the model calculations of Ref. 5. In Sec. IV we study the correlation

TABLE I. The values of $\langle n_s \rangle$, $\langle n_g \rangle$, and number of events $N_T$ for various beams and targets.

| Beam / Target | | $p_{lab}=100$ GeV/c $p$ | $\bar{p}$ | $p/\bar{p}$ | $\pi^+$ | $\pi^-$ | $\pi^+/\pi^-$ | $p_{lab}=320$ GeV/c $\pi^-$ |
|---|---|---|---|---|---|---|---|---|
| $^{24}$Mg | $\langle n_s \rangle$ | 10.23±0.67 | 10.25±0.36 | 10.25±0.32 | 9.49±0.51 | 9.17±0.29 | 9.23±0.25 | 11.79±1.22 |
| | $\langle n_g \rangle$ | 1.12±0.09 | 1.25±0.04 | 1.22±0.03 | 0.95±0.06 | 1.00±0.03 | 0.99±0.03 | 0.94±0.08 |
| | $N_T$ | 60 | 238 | 298 | 82 | 306 | 388 | 33 |
| $^{108}$Ag | $\langle n_s \rangle$ | 13.56±0.39 | 14.25±0.32 | 13.99±0.25 | 12.06±0.40 | 11.56±0.22 | 11.67±0.20 | 15.88±0.63 |
| | $\langle n_g \rangle$ | 3.21±0.07 | 3.45±0.05 | 3.36±0.04 | 2.89±0.07 | 2.65±0.04 | 2.71±0.04 | 2.83±0.08 |
| | $N_T$ | 375 | 625 | 1000 | 278 | 971 | 1249 | 246 |
| $^{197}$Au | $\langle n_s \rangle$ | 13.12±0.58 | 14.86±0.40 | 14.39±0.33 | 13.15±0.50 | 12.41±0.27 | 12.57±0.24 | 17.30±0.85 |
| | $\langle n_g \rangle$ | 3.39±0.11 | 4.07±0.09 | 3.89±0.07 | 3.64±0.10 | 3.23±0.06 | 3.32±0.05 | 3.73±0.12 |
| | $N_T$ | 187 | 522 | 709 | 234 | 800 | 1034 | 166 |

of the shower particles with the "grey" particles (mainly recoil protons). We summarize our conclusions in Sec. V.

## II. EXPERIMENTAL DATA

Our data were obtained with the Fermilab 30-in. hybrid bubble-chamber spectrometer with a downstream particle identifier. The hardware has been described elsewhere.[9] The present sample includes 5123 interactions of tagged hadrons in Mg ($A=24$), Ag ($A=108$), and Au ($A=197$) foils. All visible charged secondaries were measured. Protons, kaons, and electrons with small $p_{lab}$ have been identified by ionization; we identify most protons with $p_{lab} < 1.3$ GeV/$c$. Single δ-ray or $e^+e^-$-pair events on beam tracks have been excluded. Also excluded are events which appear to involve only $e^+e^-$ pairs or δ rays; these were selected on the basis of small average transverse momentum between the charged secondaries and the total charged-particle momentum vector. This latter exclusion is of major importance for $\pi^- A$ events because of apparent electron contamination in the beam.

It is customary to classify the secondary particles according to the track ionization they produce (i.e., the velocity $\beta$) as "black" ($\beta < 0.3$), as grey ($0.3 < \beta < 0.7$), and as shower ($\beta > 0.7$) particles. The black tracks are principally nuclear evaporation products. For the present discussion, we are interested in $n_g$, the number of grey tracks which are predominantly recoil protons,[10] and $n_s$, the number of shower particles (fast hadron secondaries) associated with hadron-nucleus interactions.

In Table I we present $\langle n_s \rangle$ and $\langle n_g \rangle$ for preliminary event samples with various beams and targets. We note that the 100-GeV/$c$ $p$ and $\bar{p}$ data have approximately the same $n_s$ distribution (not shown) within errors;[11] the same is true for the 100-GeV/$c$ $\pi^+$ and $\pi^-$ data. To improve statistics and simplify presentation we combine these samples; the $n_s$ distributions for these samples are given in Table II. In the following discussion, we show results for samples of data involving 100-GeV/$c$ $p/\bar{p}$, 100-GeV/$c$ $\pi^+/\pi^-$, and 320-GeV/$c$ $\pi^-$ beams interacting with Mg, Ag, and Au.

## III. KNO SCALING IN HADRON-NUCLEUS INTERACTIONS

In Figs. 1(a)–1(c), we plot $\Psi(z) = \langle n_s \rangle N_{n_s}/N_T$ as a function of $z = n_s/\langle n_s \rangle$ for Mg, Ag, and Au targets, respectively.[12] Here $N_{n_s}$ is the number of events with $n_s$ shower particles and $N_T$ is the total number of observed

TABLE II. Multiplicity distribution of shower particles. See Ref. 12.

| | 100-GeV/c $p/\bar{p}$ sample | | | 100-GeV/c $\pi^+/\pi^-$ sample | | |
|---|---|---|---|---|---|---|
| $n_s$ | Mg | Ag | Au | Mg | Ag | Au |
| 0–2 | 2 | 4 | 7 | 2 | 8 | 13 |
| 3–5 | 49 | 117 | 94 | 91 | 235 | 166 |
| 6–8 | 75 | 149 | 127 | 107 | 255 | 196 |
| 9–11 | 70 | 176 | 89 | 88 | 220 | 170 |
| 12–14 | 51 | 148 | 86 | 52 | 167 | 135 |
| 15–17 | 24 | 123 | 72 | 19 | 134 | 113 |
| 18–20 | 15 | 90 | 70 | 20 | 75 | 84 |
| 21–23 | 2 | 72 | 60 | 4 | 71 | 57 |
| 24–26 | 7 | 51 | 31 | 2 | 37 | 42 |
| 27–29 | 2 | 26 | 25 | 3 | 24 | 27 |
| 30–32 | 1 | 23 | 26 | | 13 | 16 |
| 33–35 | | 11 | 9 | | 6 | 11 |
| 36–38 | | 5 | 7 | | 4 | 2 |
| 39–41 | | 2 | | | | 1 |

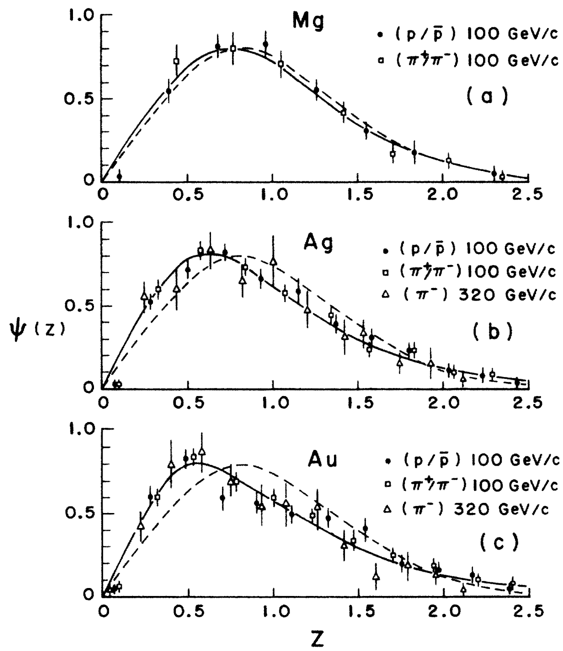


FIG. 1. Plots of $\Psi(z)=\langle n_s\rangle N_{n_s}/N_T$ as a function of $z=n_s/\langle n_s\rangle$. The dashed curve corresponds to the Slattery function and the solid curves correspond to the prediction of the model of Ref. 5: (a) for $h$-Mg interactions, (b) for $h$-Ag interactions, and (c) for $h$-Au interactions.

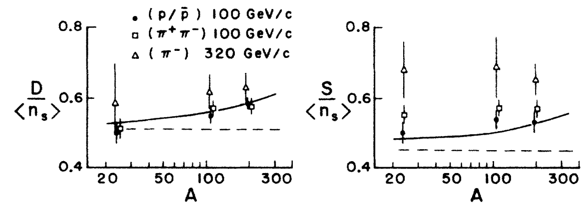


FIG. 2. (a) Plot of $D/\langle n_s\rangle$ ($D$ is dispersion) as a function of $A$. (b) Plot of $S/\langle n_s\rangle$ ($S$ is skewness) as a function of $A$. The dashed and solid curves are the predictions from the Slattery curve and the model of Ref. 5, respectively.

events. The dashed curves shown here correspond to the KNO scaling function obtained by Slattery[13] for hadron-hadron interactions. While no significant differences can be seen for different incident hadrons or for different energies,[14] the experimental data clearly deviate from the Slattery curve.[15] The data peak at a lower value of $z$ than that given by the dashed curve, the effect becoming more pronounced for heavier nuclei. A possible explanation of the observed effect is given by Kiang, Ling, Young, and Lam.[5] The solid curves in Fig. 1 have been calculated using this model. The calculated results are in excellent agreement with the data. The behavior of the dispersion

$$D=\langle (n_s-\langle n_s\rangle)^2\rangle^{1/2}$$

and skewness

$$S=\langle (n_s-\langle n_s\rangle)^3\rangle^{1/3}$$

as a function of $A$ are shown in Figs. 2(a) and 2(b). Here again, the data do not agree with the constant values predicted from the Slattery function (dashed curve) but are reasonably consistent with the type of variation indicated by the solid curves obtained from the model.

We briefly sketch the calculations involved in the model of Ref. 5. Let $n_{hA}$ be the number of shower particles produced in $h$-$A$ collisions and $n_{hN}$ be the number of shower particles produced in $h$-$N$ collisions at the same energy. (For the present discussion $n_{hA}$ is the same as our $n_s$.) In addition to the parameter $z=n_{hA}/\langle n_{hA}\rangle$ defined above, a corresponding parameter $z_{hN}=n_{hN}/\langle n_{hN}\rangle$ is defined for hadron-nucleon interactions and is used in the Slattery parametrization. The experimental data can be described[4] by

$$\langle n_{hA}\rangle=[1+\beta(\nu_A-1)]\langle n_{hN}\rangle\ , \tag{1}$$

where $\beta\approx 0.4$–$0.6$; $\nu_A=A\sigma_{hN}/\sigma_{hA}$ is the average number of hadron-nucleon collisions in nucleus $A$. If one assumes that $n_{hA}$ is also related to $n_{hN}$ by the same expression, then $z=z_{hN}$; in such a case, the KNO scaling function for hadron-nucleus interactions $\Psi(z)$ would be identical with the Slattery scaling function $\Psi_{\rm Sl}(z_{hN})$.

In Ref. 5, it is assumed that the multiplicity distribution obeys universal KNO scaling at each impact parameter $b$. Let $\nu(b)$ be the number of hadron-nucleon collisions for fixed impact parameter $b$, and $n_{hA}(b)$ be the corresponding number of shower particles produced. One then defines $z(b)=n_{hA}(b)/\langle n_{hA}\rangle$. Using Eq. (1), one can write

$$z(b)=\frac{1+\beta[\nu(b)-1]}{1+\beta(\nu_A-1)}\frac{n_{hN}}{\langle n_{hN}\rangle}\equiv q(b)z_{hN}\ . \tag{2}$$

Then one can relate the hadron-nucleus KNO function $\Psi_b(z)$ for a fixed impact parameter $b$ to the Slattery function using $\Psi_b(z)dz=\Psi_{\rm Sl}(z_{hN})dz_{hN}$ to obtain

$$\Psi_b(z)=[1/q(b)]\Psi_{\rm Sl}(z/q(b))\ . \tag{3}$$

The weighted multiplicity distribution for a fixed impact parameter is then finally written as

$$\Psi_b'(z)=d^2b\{1-\exp[-\sigma t(b)]\}\Psi_b(z)\ , \tag{4}$$

where $t(b)$ is the thickness of the target at impact parameter $b$ and $\sigma$ is the hadron-nucleon interaction cross section. The quantity $\nu(b)$ appearing in $q(b)$ is also related to $t(b)$ via

$$\nu(b)=\sigma t(b)/\{1-\exp[-\sigma t(b)]\}\ . \tag{5}$$

We average the function of Eq. (4) over all $b$ for a given nucleus to obtain the functions $\Psi(z)$ which have been plotted in Fig. 1. The dependence of the KNO-scaled multiplicity distributions on $A$ results only when the elementary distribution [Eq. (3)] is convoluted over all impact parameters.

## IV. CORRELATION OF SHOWER AND GREY PARTICLES

We may also study the dependence of $\langle n_s'\rangle\equiv\langle n_s(n_g)\rangle$ on $n_g$, where $n_g$ is the number of grey particles (mainly recoil protons). In Table III we present $\langle n_s'\rangle$ for various values of $n_g$ for the 100-GeV/$c$ data. These data show that $\langle n_s' \rangle$ increases with $n_g$ for a given value of $A$. In the following we show that this feature can be quantitatively understood from the model of Ref. 5.

In Eq. (5), we see that $\nu$ is uniquely related to $b$ and hence the multiplicity distribution can be evaluated as a function of $\nu$. As we calculate $\Psi_b'(z)$ by varying $b$ in steps over the entire $b$ range for a given nucleus, we histogram the values of $\Psi_b'$ and $z\Psi_b'$ as a function of $z$ for a fixed $\nu$ interval. One can then calculate $\langle z(\nu) \rangle$ by using $\langle z(\nu) \rangle = (\sum z\Psi_b' / \sum \Psi_b')$. Since $z(\nu) = n_s(\nu)/\langle n_s \rangle$, where $\langle n_s \rangle$ refers to the overall average multiplicity, the value of $n_s(\nu)$ is readily obtained from the relation $\langle n_s(\nu) \rangle = \langle z(\nu) \rangle \langle n_s \rangle$. In Fig. 3(a), we plot the calculated $n_s(\nu)$ as a function of $\nu$ for $p/\bar{p}$ beams.

Experimentally one cannot readily study the multiplicity distribution as a function of the number of collisions. It is now necessary to relate $\nu$ to $n_g$ in order to compare the experimental data with the calculations. Andersson, Otterlund, and Stenlund[16] have proposed that the number of projectile collisions is related to the production of grey particles. In Fig. 3(b), we show their results calculated for $A = 14$, 40, and 108. In Fig. 3(c), we present $\langle n_s' \rangle$ as a function of $n_g$ for $(p/\bar{p})$Ag and $(\pi^+/\pi^-)$Ag interactions. The curves correspond to the model calculations of Fig. 3(a) plotted as a function of $n_g$ using the $\nu$-$n_g$ relationship shown in Fig. 3(b) for $A = 108$. The increase of $\langle n_s' \rangle$ with $n_g$ is well described by the model.

## V. SUMMARY

We have presented data on charged-particle multiplicity distributions in hadron-nucleus interactions involving nuclei of different mass number $A$. We observe clear dependence of the KNO-scaled multiplicity distributions on $A$. Our data are compared with a model[5] which derives the multiplicity distributions in hadron-nucleus interactions by convoluting the KNO-scaled hadron-hadron multiplicity distribution for various impact parameters, and predicts $A$ dependence for the overall multiplicity distributions. Using this model and the work of Andersson, Otterlund, and Stenlund,[16] we have calculated the correlation between the production of shower particles and that of grey particles. The predictions of the model agree well with the experimental data.

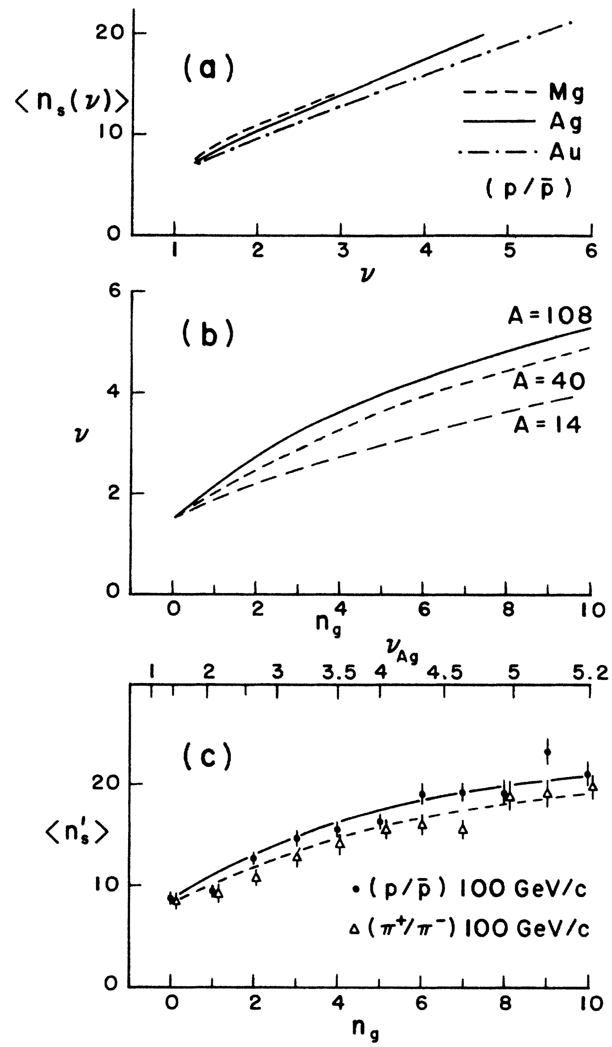


FIG. 3. (a) Mean shower-particle multiplicity $\langle n_s(\nu) \rangle$ as a function of $\nu$ from the model of Ref. 5. (b) Relationship between $\nu$ and $n_g$ calculated in Ref. 16. (c) The dependence of $\langle n_s' \rangle$ on $n_g$ for our 100-GeV/$c$ data. The curves shown here are obtained from the calculations shown in (a) and (b). The solid curve corresponds to $p/\bar{p}$ beams (with $\sigma_{hh} = 32$ mb) and the dashed curve corresponds to $\pi^+/\pi^-$ beams (with $\sigma_{hh} = 20$ mb).

TABLE III. Values of $n_s'$ for various values of $n_g$.

| | $\langle n_s' \rangle$ for 100-GeV/$c$ $p/\bar{p}$ data | | | $\langle n_s' \rangle$ for 100-GeV/$c$ $\pi^+/\pi^-$ data | | |
|---|---|---|---|---|---|---|
| $n_g$ | Mg | Ag | Au | Mg | Ag | Au |
| 0 | 8.70±0.35 | 8.80±0.27 | 8.26±0.30 | 8.56±0.28 | 7.76±0.20 | 8.09±0.22 |
| 1 | 9.59±0.58 | 9.65±0.39 | 9.75±0.56 | 8.99±0.50 | 9.34±0.31 | 9.48±0.35 |
| 2 | 12.67±1.06 | 12.83±0.48 | 14.45±0.84 | 10.36±0.86 | 11.66±0.48 | 11.29±0.56 |
| 3 | 13.10±1.46 | 14.71±0.66 | 13.79±1.04 | 10.35±1.00 | 13.20±0.56 | 12.75±0.71 |
| 4 | 15.58±0.88 | 15.84±0.69 | 16.16±1.11 | 11.91±1.80 | 14.70±0.78 | 14.98±0.91 |
| 5 | | 16.59±0.84 | 15.88±1.07 | | 15.66±0.82 | 14.02±0.95 |
| 6 | | 19.54±1.05 | 20.57±1.19 | | 16.29±1.12 | 16.68±1.20 |
| 7 | | 19.16±1.20 | 18.96±1.30 | | 16.13±1.20 | 18.62±2.26 |
| 8 | | 19.94±1.30 | 18.58±1.50 | | 19.31±1.71 | 19.94±1.72 |
| 9 | | 23.64±1.60 | 22.52±1.70 | | 19.94±1.65 | 18.00±1.96 |
| 10 | | 21.58±2.30 | 22.92±1.90 | | 21.81±2.36 | 22.27±2.16 |

## ACKNOWLEDGMENTS

We gratefully acknowledge the efforts of the scanning, measuring, and technical staffs of the collaborating institutions. Particular thanks are due to Kathleen DeLanghe for her essential work in identifying secondaries and in putting the data in usable form at Notre Dame and to the measuring staffs of Cambridge and Notre Dame for their painstaking measurement of the complex nuclear interactions. We thank the staffs of the accelerator and 30-in. bubble chamber at Fermilab for their contributions to the experiment. This work was supported in part by the U.S. National Science Foundation (Notre Dame, Kansas, Pennsylvania State), U.S. Department of Energy (Duke, Fermilab), and the U.K. Science and Engineering Research Council (Cambridge).


---


[1]A. Azimov *et al.*, Phys. Rev. D **23**, 2512 (1981).

[2]V. H. Areti *et al.*, Phys. Rev. D **15**, 1874 (1977); F. Takagi, Prog. Theor. Phys. **62**, 457 (1979).

[3]Z. Koba, H. B. Nielsen, and P. Olesen, Nucl. Phys. **B40**, 317 (1972).

[4]E. R. Nakamura, M. Murayama, and A. Nakamura, Phys. Rev. D **27**, 1457 (1983); see also references therein.

[5]D. Kiang, S. H. Ling, K. Young, and C. S. Lam, Phys. Rev. D **31**, 31 (1985).

[6]J. R. Florian *et al.*, Phys. Rev. D **13**, 558 (1976); S. A. Azimov *et al.*, Yad. Fiz. **30**, 1033 (1979) [Sov. J. Nucl. Phys. **30**, 537 (1979)].

[7]M. A. Faessler *et al.*, Nucl. Phys. **B157**, 16 (1979).

[8]C. DeMarzo, *et al.*, Phys. Rev. D **26**, 1019 (1982).

[9]W. D. Shephard *et al.*, in *Multiparticle Dynamics, 1983,* proceedings of the XIV International Symposium, Lake Tahoe, edited by J. F. Gunion and P. M. Yager (World Scientific, Singapore, 1983); J. Whitmore *et al.*, in *Multiparticle Dynamics, 1982,* proceedings of the XIII International Symposium, Volendam, The Netherlands, edited by W. Kittel, W. Metzger, and A. Stergiou (World Scientific, Singapore, 1983), p. 359.

[10]For grey tracks ($0.3<\beta<0.7$), the momentum range is from 0.29 to 0.92 GeV/$c$ for protons and from 0.04 to 0.14 GeV/$c$ for pions. Thus it is necessary to identify tracks up to $p \approx 1$ GeV/$c$ for proper classification of the tracks. In the present experiment, ionization identification has been possible up to $p=1.3$ GeV/$c$; in contrast, this has been possible only up to $p=0.6$ GeV/$c$ in streamer-chamber experiments (Ref. 8) and hence the protons with $\beta>0.54$ in those experiments were classified as shower particles.

[11]Table I shows, e.g., slightly larger values of $\langle n_s \rangle$ and $\langle n_g \rangle$ for $\bar{p}$-Au than for $p$-Au interactions at 100 GeV/$c$. While these small differences may be significant, they do not result in significant differences in the scaled multiplicity distributions at the present level of statistics.

[12]For the present study, identified $e^{\pm}$ have been excluded from the secondaries but no other corrections (for, e.g., unidentified electrons or unobserved secondary interactions and decays near the vertex) have been made. The effect of such corrections would be to lower slightly the $\langle n_s \rangle$ values, especially for larger-$A$ nuclei. We do not expect such corrections to change the distributions of Fig. 1 significantly.

[13]P. Slattery, Phys. Rev. Lett. **29**, 1624 (1972).

[14]Although no differences in the distributions of Fig. 1 as a function of incident energy are obvious at the present level of statistics, we note that the multiplicity distribution for 320-GeV/$c$ $\pi^- A$ interactions extends to higher values of $n_s$ than those for 100-GeV/$c$ $(\pi^+/\pi^-)A$, resulting in somewhat larger values for the moments.

[15]We have also studied the distributions for negative and positive shower particles separately. They are consistent with each other and with the total-$n_s$ KNO distributions, and show similar deviations from the Slattery curve even though the positive samples included all protons with $\beta>0.7$.

[16]B. Andersson, I. Otterlund, and E. Stenlund, Phys. Lett. **73B**, 343 (1978).